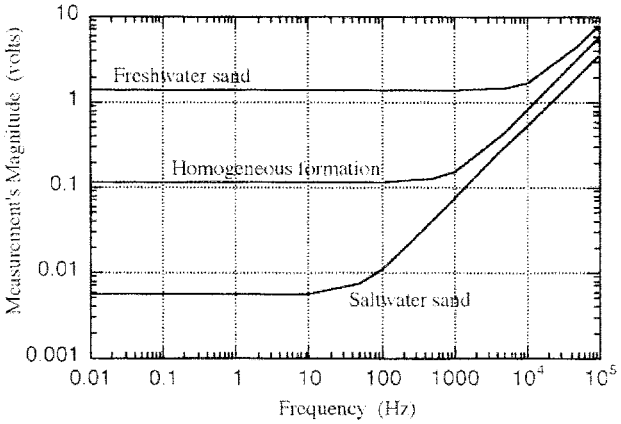

Fig. 3. Frequency response of a simple logging device.

the curves present a constant behavior at low frequencies and at relatively high frequency values they increase with frequency. It can be verified that the points at which the curves start to deviate from the constant line are related to those frequency values at which the skin depth in the formation becomes comparable to the length of the tool.

It can be concluded from these results that in the typical range of operational frequencies, which is between 10 and 100 Hz for such type of devices, the measurement is substantially affected only for the case of the saltwater sand formation.

VI. Conclusion

The time-harmonic field analysis procedure presented here constitutes a new methodology that presents some important advantages over the conventional direct-current analysis techniques. It allows one to study the electric logging systems at their real frequencies of operation without the necessity of electrostatic assumptions.

As may be concluded from the simulation results, the validity of the electrostatic assumption cannot be always presupposed. In particular, special care must be exercised when dealing with conductive formations.

The presented time harmonic field analysis procedure also provides a means for studying the suitability of frequency-based radial resistivity sounding.

References

[1] J. Hallenburg, *Geophysical Logging for Mineral and Engineering Applications*. New York: Wiley, 1984.

[2] J. Lovell and W. Chew, "Response of a point source in a multicylindrically layered medium," *IEEE Trans. Geosci. Remote Sensing*, vol. GE-25, pp. 850–858, 1987.

[3] M. Moghaddam, "Response of a vertical magnetic dipole in cylindrically stratified media," Masters thesis, Univ. of Illinois at Urbana-Champaign, 1989.

[4] W. Chew, "Response of a current loop antenna in an invaded borehole," *Geophys.*, vol. 49, no. 1, pp. 81–91, 1984.

[5] W. Chew, S. Barone, B. Anderson, and C. Hennessy, "Diffraction of axisymmetric waves in a borehole by bed boundary discontinuities," *Geophys.*, vol. 49, no. 4, pp. 1586–1595, 1984.

[6] W. Chew, Z. Nie, Q.-H. Liu, and B. Anderson, "An efficient solution for the response of electrical well logging tools in a complex environment," *IEEE Trans. Geosci. Remote Sensing*, vol. 29, pp. 308–313, 1991.

[7] Q.-H. Liu, "Electromagnetic field generated by an off-axis source in a cylindrically layered medium with an arbitrary number of horizontal discontinuities," *Geophysics*, vol. 58, no. 5, pp. 616–625, 1993.

[8] F. X. Bostick and H. Smith, "Propagation effects in electric logging," Internal Rep., Dept. Elect. Comput. Eng., Univ. Texas, Austin, 1994.

[9] M. Goldman, *Non-Conventional Methods in Geoelectrical Prospecting*. London, U.K.: Ellis Horwood, 1990.

[10] V. Sokolov and L. Tabarovsky, "On calculating electromagnetic fields for induction logging problems by deformation of the integration path into the complex plane of the integration variable," *Geol. Geofiz.*, vol. 3, pp. 86–93, 1973.

[11] W. Anderson, "Numerical integration of related Hankel transforms of orders 0 and 1 by adaptive digital filtering," *Geophys.*, vol. 44, no. 7, pp. 1287–1305, 1979.

[12] A. Chave, "Numerical integration of related Hankel transforms by quadrature and continued fraction expansion," *Geophysics*, vol. 48, no. 12, pp. 1671–1686, 1983.

[13] J. Moore and R. Pizer, *Moment Methods in Electromagnetics*. New York: Wiley, 1984.

Modeling Non-Rayleigh Speckle Distribution in SAR Images

Yves Delignon and Wojciech Pieczynski

***Abstract*—In non-Rayleigh distributed radar images, the number of scatterers can be viewed as a Poisson distributed random variable, with the mean itself random. When this mean is Gamma distributed, then the image classically satisfies the K distribution. We add three new possible distributions for this mean: inverse Gamma, Beta of the first kind, and Beta of the second kind. We show that new intensity distributions so obtained can be estimated, with the interest of the extension validated on a real image.**

***Index Terms*—K law, Pearson system, scatterer, speckle, statistical modeling of SAR images.**

I. Introduction

In radar imagery, the observed intensity is the sum of the contributions of the different scatterers at the observed surface. In the classical approach, the number of scatterers in each elementary cell is assumed to be large enough and approximately constant. The reflected electrical field is then Gaussian; the observed intensity admits an exponential distribution, and the amplitude admits a Rayleigh one. However, when the number of scatterers varies, the distribution of the resulting field may be non-Gaussian, and so the observed intensity may no longer be exponential. Assuming that the random number of scatterers in each elementary cell is distributed according to a Poisson distribution, one can consider that the mean of this distribution, or the "expected number of scatterers," is itself a random variable [14]. It is well known that when this random variable is Gamma distributed, the intensity of the back-scattered field is K distributed [2]–[7], [12]–[15], [17], [20], [22], [27]. In this paper, we extend the possibilities of distributions of this expected number of scatterers to three new distributions—inverse Gamma, Beta of the first kind, or Beta of the second kind—and show that the intensity distribution of the back-scattered field can be calculated in these three new cases. Furthermore, we propose a method of classification, using only the observed image, in which case, among four possibilities

Manuscript received January 23, 2001; revised October 31, 2001.

Y. Delignon is with the Département Electronique, Ecole Nouvelle d'Ingénieurs en Communication, 59658 Villeneuve d'Ascq, France (e-mail: Yves.Delignon@enic.fr).

W. Pieczynski is with the Département CITI, Institut National des Télécommunications, 91000 Evry, France (e-mail: Wojciech.Pieczynski@int-evry.fr).

Publisher Item Identifier 10.1109/TGRS.2002.800234.

including the classical case and the three new cases, the observed intensity data lie. The usefulness of the three new distributions is tested on a real image, and it turns out that there exist situations in which the new distributions are of interest.

This article is organized as follows. In Section II, we briefly recall the Pearson system of distributions and specify the four distributions of the intensity corresponding to four distributions of the expected number of scatterers. Section III is devoted to the problem of intensity identification, which consists of finding simultaneously the form of its distribution and the corresponding parameters. In Section IV, we present some experimental results. Our conclusions and some perspectives for further work are presented in Section V.

II. Intensity Distribution

Let us consider the propagation in free space of an incident monochromatic wave on a rough surface, with the surface variation much larger than the wavelength. The back-scattered field from an illuminated area takes the form

$$F = \sum_{k=1}^{n} F_k = \sum_{k=1}^{n} A_k e^{i\theta_k} \tag{1}$$

where n is the number of scatterers, A_k is the amplitude, and θ_k is the phase of the kth component. $A_1, \ldots, A_n$ will be assumed to be independent random variables with the same distribution and likewise for $\theta_1, \ldots, \theta_n$, each of which has a uniform distribution on [0, 2π].

If n is large and constant, we get a circular Gaussian distribution for the back-scattered field. Its components are independent, zero mean and have the same variance $n\sigma^2$, where σ^2 is the common variance of $A_1, \ldots, A_n$. Consequently, the amplitude is Rayleigh distributed, and the intensity obeys an exponential law with parameter $1/n\sigma^2$ [10], [25]. When the number n of scatterers is random, it can be considered as a realization of a Poisson distributed random variable N, with $E[N] = \lambda$. Let λ itself be a realization of a random variable Λ. So the distribution of Λ defines the distribution of N, which defines the distribution of F. We assume that the distribution of Λ has a density f, and our aim is to seek f from the observed image. We assume that f is in Pearson's system of distributions, which covers a large variety of density shapes [7], [16]. Since Λ is a positive variable, we select the Pearson densities having a positive support. This is why only three coefficients are used in (2), instead of four generally taken. The Pearson system contains a great number of known parametric laws, from which we have chosen four laws as possible distributions for Λ: the Gamma distribution, Beta distribution of the second kind, the inverse Gamma distribution, and Beta distribution of the first kind. Let us recall that the Pearson distribution system is defined as containing the densities verifying the differential equation (2), the variations of a, c_1, c_2 providing different distributions:

$$\frac{df(x)}{f(x)} = -\frac{x+a}{x\,(c_1 + c_2 x)}dx,\ x > 0. \tag{2}$$

Now, let us consider the first four moments $m_1 = \int_R x f(x)dx$ and $m_i = \int_R (x - m_1)^i f(x)dx$ for $2 \le i \le 4$, and let us denote by β_1 and β_2 the following functions:

$$\beta_1 = \frac{(m_3)^2}{(m_2)^3},\ \beta_2 = \frac{m_4}{(m_2)^2} \tag{3}$$

($\sqrt{\beta_1}$ is called "skewness," and β_2 is called "kurtosis"). According to the general theory, β_1 and β_2 define a unique density f in the Pearson system, and f can be analytically specified from them. Otherwise, it is possible to show, that if λ is large enough, the distribution of the field F conditional to $\Lambda = \lambda$ is circular Gaussian with variances of real and imaginary parts equal to $\lambda\sigma^2/2$, and so the distribution of the random intensity I conditional to $\Lambda = \lambda$ is an exponential distribution of parameter $\lambda\sigma^2$. This implies the following relation among the moments of Λ and the moments of I [19]:

$$E\left[I^k\right] = \sigma^{2k}\Gamma(k+1)E\left[\Lambda^k\right]. \tag{4}$$

Important for what follows is that it is then possible to estimate β_1 and β_2 from I. In fact, the moments $m_1, \ldots, m_4$ can be calculated from $E[\Lambda^1], \ldots, E[\Lambda^4]$, and the latter can be calculated from $E[I^1], \ldots, E[I^4]$ and σ^2 using (4). Now, when applying (3), σ^2 disappears; thus β_1 and β_2 are expressed as functions of $E[I^1], \ldots, E[I^4]$, the latter being easily estimated from I by $\hat{E}[I^i] = ((x_1)^i + \cdots + (x_1)^i)/n$, where $x_1, \ldots, x_n$ are the observed intensity values on different pixels corresponding to a given class.

Let us note, that according to (3), we must have $m_2 \neq 0$, the case $m_2 = 0$ corresponding to a constant λ and thus to an exponential density. The latter case is easily detected because in the exponential case we have $E[I] = Var[I]$ and so

$$E[I] = E\left[I^2\right] - (E[I])^2. \tag{5}$$

So we first look at (5), and if it is verified, λ is a constant (the distribution of Λ is a Dirac distribution).

Finally, when λ is not a constant and f is the density of the distribution of Λ, (β_1, β_2) can be estimated from the observed sample of I and thus gives the distribution of Λ, when the latter is in the Pearson system.

Furthermore, if the distribution of Λ is among the four distributions mentioned above, it is possible to calculate the corresponding distribution of I. In fact, if f is the density of the distribution of Λ and g is the density of the distribution of I, recalling that the distribution of I conditional to $\Lambda = \lambda$ is an exponential distribution of parameter $\lambda\sigma^2$, we have the following:

$$g(x) = \int_0^{+\infty} \frac{1}{\lambda\sigma^2} e^{-x/\lambda\sigma^2} f(\lambda)d\lambda. \tag{6}$$

The integral (6) can be evaluated in the following four cases, of which the first is well known:

1) f is a Gamma distribution:

$$f(x) = cx^{\alpha-1}\exp\left[-\frac{x}{\beta}\right],\ x \in [0, +\infty) \tag{7}$$

with $c = 1/\beta^\alpha\Gamma(\alpha)$ (with Γ the Gamma function [1]), $\alpha = -a/c_1 + 1$, and $\beta = c_1$. g is then defined by the following "K density" [14]:

$$g(x) = c'\left(\frac{x}{\sigma^2\beta}\right)^{(\alpha-1)/2} K_{\alpha-1}\left(2\sqrt{\frac{x}{\sigma^2\beta}}\right),\ x \in [0, +\infty) \tag{8}$$

where K is the modified Bessel special function of the second kind [1] and $c' = 2/\Gamma(\alpha)\sigma^2\beta$. Concerning this classical case, let us mention that first studies were performed by Jakeman *et al.* [12]–[14]. Afterward, Oliver proposed correlated K distribution [22]; Jao used K distribution in the case of rural illuminated [15]; Barakat obtained K distributions in case of weak scattering [2], [3], and Yueh and Kong [27] created an extension of K distribution for multipolarization images.

2) f is the Beta distribution of the second kind:

$$f(x) = c\frac{x^{p-1}}{(x+\beta)^{p+q}},\ x \in [0, +\infty) \tag{9}$$

with $p = -a/c_1 + 1$, $q = 1/c_2 - 1$, $\beta = c_1/c_2$, and $c = \beta^q/B(p, q)$ (with $B(p, q)$ the Beta function [1]). g is then given by the following "U distribution" [6], [14]:

$$g(x) = c'U_{q+1,2-p}\left(\frac{x}{\sigma^2\beta}\right),\ x \in [0, +\infty) \tag{10}$$

with $c' = q\Gamma(p+q)/\sigma^2\beta\Gamma(p)$. The function U is also called the "degenerate hypergeometric function" [1].

TABLE I
CORRESPONDENCE BETWEEN Λ AND I DISTRIBUTIONS

Λ distribution	Gamma	Beta second kind	inverse Gamma	Beta first kind	Dirac
I distribution	K	U	B	W	Exponential

3) f is the inverse Gamma distribution:

$$f(x) = c\frac{1}{x^{\alpha+1}}\exp\left[-\frac{\beta}{x}\right],\ x \in (0,+\infty) \tag{11}$$

with $c = \beta^\alpha/\Gamma(\alpha)$, $\alpha = 1/c_2$, and $\beta = -a/c_2$. g is then the Beta distribution of the second kind (B) [19]:

$$g(x) = c'\frac{1}{(x+\sigma^2\beta)^{\alpha+1}},\ x \in [0,+\infty) \tag{12}$$

with $c' = \alpha(\sigma^2\beta)^\alpha$. This result is quite interesting, as it has previously been suggested in [21] and, in another procedure of statistical modeling, in [6].

4) f is Beta distribution of the first kind:

$$f(x) = cx^{p-1}(\beta - x)^{q-1},\ x \in [0,\beta] \tag{13}$$

with $p \geq 0$, $q \geq 0$, and $\beta > 0$.

g is then defined by the W density [6], [20]:

$$g(x) = c'\left(\frac{x}{\sigma^2\beta}\right)^{(p/2)-1} \cdot \exp\left[-\frac{x}{2\sigma^2\beta}\right] W_{(-p-2q+2)/2,\,(p-1)/2}\left(\frac{x}{\sigma^2\beta}\right) \tag{14}$$

with $c' = \Gamma(p+q)/\Gamma(p)\sigma^2\beta$, $p = -a/c_1+1$, $q = a/c_1-1/c_2+1$, $\beta = -c_1/c_2$, and W the Whittaker special function [1].

These four cases are summarized in Table I.

Finally, let us specify how the nature of the Λ distribution is defined from β_1 and β_2 given by (3). Putting

$$A = \frac{\beta_1(\beta_2+3)^2}{4(4\beta_2-3\beta_1)(2\beta_2-3\beta_1-6)} \tag{15}$$

we have, for P_Λ, the distribution of Λ:

$$\begin{aligned}
(P_\Lambda \text{ is Gamma}) &\Leftrightarrow 2\beta_2 - 3\beta_1 - 6 = 0;\\
(P_\Lambda \text{ is Beta second kind}) &\Leftrightarrow A > 1;\\
(P_\Lambda \text{ is inverse Gamma}) &\Leftrightarrow A = 1;\\
(P_\Lambda \text{ is Beta first kind}) &\Leftrightarrow A < 0.
\end{aligned} \tag{16}$$

III. INTENSITY ESTIMATION

The aim of this section is to specify how to estimate the distribution of I. Choosing a sample of intensities $I_1, \ldots, I_n$ on n pixels, let $\hat{\mu}_1, \ldots, \hat{\mu}_4$ be the empirical estimates, obtained from $I_1, \ldots, I_n$, of the first four moments of the distribution of I. As specified above, these moments allow us to calculate β_1, β_2, which give the nature of the distribution of Λ. Assuming that this nature is one of cases 1–4, we have to estimate the corresponding parameters. In cases 1 and 4, the distributions "W" and "U" are defined by three parameters: $\gamma = \beta\sigma^2$, p, and q; and in cases 2 and 3, the distributions "K" and "B" are defined by two parameters: $\gamma = \beta\sigma^2$ and α. Putting

$$a = \frac{\hat{\mu}_2}{2(\hat{\mu}_1)^2},\ b = \frac{\hat{\mu}_3}{3\hat{\mu}_1\hat{\mu}_2} \tag{17}$$

TABLE II
ESTIMATES OF THE FOUR POSSIBLE DISTRIBUTIONS OF I FROM EMPIRICAL MOMENTS a AND b DEFINED BY (17)

Law of I	$\hat{\gamma}$	$\hat{p}$	$\hat{q}$	$\hat{\alpha}$
K	$\hat{\mu}_1(a-1)$			$\frac{1}{a-1}$
U	$\hat{\mu}_1\frac{b(a-2)+a}{2a-b-1}$	$\frac{2(a-b)}{b(2-a)-a}$	$\frac{4a-3b-1}{2a-b-1}$	
B	$\hat{\mu}_1$			$\frac{a+1}{a}$
W	$\hat{\mu}_1\frac{b(a-2)+a}{2a-b-1}$	$\frac{2(a-b)}{b(2-a)-a}$	$\frac{2(a-b)(a-1)(b-1)}{(2a-b-1)(2b-ab-a)}$	

the possible estimates of γ, p, q, and α corresponding to different cases 1–4 are presented in Table II.

Finally, when the distribution of I lies in the set $\Delta = \{K, U, B, W\}$, which we will call the "*KUBW* system," its identification can be done in three steps.

1) Estimate the four first moments $\mu_1, \ldots, \mu_4$ of the distribution of I, and calculate $m_1, \ldots, m_4$ with (4) and β_1, β_2 with (3).
2) Identify the distribution of Λ in the Pearson system with (15) and (16) and using Table I find the distribution of I in the *KUBW* system.
3) Estimate the parameters of the distribution of I using (17) and Table II.

So, when the distribution of I is in the *KUBW* system, we obtain an automated procedure to find its nature and to estimate its parameters.

Remark 3.1: The calculations above are based on the fact that the distribution of the field F conditional to $\Lambda = \lambda$ is circular Gaussian with variance of the amplitude equal to $\lambda\sigma^2$. Otherwise, we also mentioned that for the number of scatterers $N = n$ large enough and approximately constant, the distribution of the field F conditional to σ^2 is circular Gaussian with variance of the amplitude equal to $n\sigma^2$. The latter case has been studied in [5], where σ^2 was assumed to be random. In an analogous manner, when the distribution of σ^2 is Gamma, Beta of the second kind, inverse Gamma, or Beta of the first kind, the distribution of I is K, U, B, and W, respectively. However, these two situations are "physically" different: in this paper σ^2 is constant, which means that the nature of the scatterers is the same in the whole image. For example, if we have the same kind of trees in the whole image and the density per pixel of those trees varies, then variations of the shape of the intensity distribution can be due to the variation of the distribution of Λ—as described in this paper—and cannot be due to any variation of σ^2 which, only depending on the kind of trees, is constant. Finally, this remark allows us to consider the following "mixed" case, which undoubtedly is more frequent in real situations: both n and σ^2 are realizations of random variables N and Σ^2. Then all results presented in this paper remain valid once we show that the distribution of the field F conditional to $N\Sigma^2 = n\sigma^2$ is Gaussian. Thus, when the distribution of $N\Sigma^2$ is Gamma, Beta of the second kind, inverse Gamma, or Beta of the first kind, the distribution of I is K, U, B, and W, respectively.

IV. EXPERIMENTS

We present below different results concerning a three-look amplitude JERS1 image of Rondonie, whose resolution is 25 m × 25 m and which contains four classes (see Figs. 1 and 2). Rondonie is a part of the Amazon where cultivation displaces the forest. In the Amazon, the prevalent method of cultivation, called "slash and burn," is made in the following way: first plots of dense forest are cut and burned. Then, plots of burnt land are put into cultivation and converted into meadows after two or three years. Then other plots of forest are cut, burned, and transformed into cultivated land. Finally, we have four classes: burn plot, cultivation, dense forest, and recent pasture.

Fig. 1. Three-look image JERS1 of Rondonie.

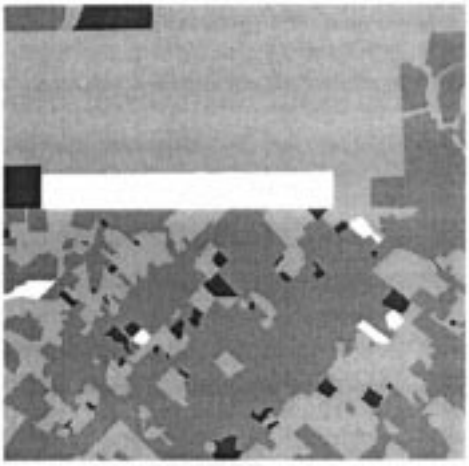

Fig. 2. Image of classes: burned plot, cultivation, dense forest, recent pasture.

Thus we have, in the image considered, $A = \sqrt{I} = ((I_1 + I_2 + I_3)/3)^{1/2}$, where the random intensities I_1, I_2, and I_3 have a common distribution assumed to be K, U, B, or W. To decide in which case the data lie, we have to calculate, according to the previous section, $E[(I_1)^i]$, for $1 \leq i \leq 4$. As $E[(I_1)^i] = E[(I_2)^i] = E[(I_3)^i]$ and $E[(I)^i] = E[(I_1 + I_2 + I_3)^i]/3$, all $E[(I_1)^i]$ can be easily calculated from the four $E[(I)^i]$, the latter being estimated from the samples $I_1 = (A_1)^2, \ldots, I_n = (A_n)^2$ (remember that four different samples, corresponding to the four classes, are used).

Remark 4.1: The distribution of I is here the convolution product of the distributions of $I_1/3$, $I_2/3$, and $I_3/3$, and thus it can no longer remain in the K, U, B, W system. However, in each of these four cases its density g is calculable. In fact, if we have n looks ($n = 3$ here), the K, U, B, and W densities given by (8), (10), (12), and (14), respectively, become as follows:

$$g(x) = \frac{2}{\Gamma(n)\Gamma(\alpha)\sigma^2\beta}\left(\frac{x}{\sigma^2\beta}\right)^{(\alpha+n-2)/2} \cdot K_{\alpha-n}\left(2\sqrt{\frac{x}{\sigma^2\beta}}\right), \tag{18}$$

$$g(x) = \frac{\Gamma(n+q)}{\Gamma(n)B(p,q)\sigma^2\beta}\left(\frac{x}{\sigma^2\beta}\right)^{n-1} \cdot U_{q+n,1+n-p}\left(\frac{x}{\sigma^2\beta}\right), \tag{19}$$

TABLE III
ESTIMATED $\boldsymbol{\lambda}$ AND $\boldsymbol{I}$ DISTRIBUTIONS WITH CORRESPONDING PARAMETERS

	Class 1 (Burnt plot)	Class 2 (Cultivation)	Class 3 (Dense forest)	Class 4 (Recent pasture)
Λ *law*	Beta of the first kind	Beta of the second kind	Constant	Beta of the second kind
I *law*	W	U	exponential	U
p	1.913	2.780	-	2.978
q	0.205	6.919	-	31.515
γ	15385	8718.2	-	73186
d	**1.278**	**6.375**	**-**	**2.433**

$$g(x) = \frac{(\sigma^2\beta)^\alpha x^{n-1}}{B(n,\alpha)(x+\sigma^2\beta)^{\alpha+n}} \tag{20}$$

$$g(x) = \frac{\Gamma(q)}{\Gamma(n)B(p,q)\sigma^2\beta}\left(\frac{x}{\sigma^2\beta}\right)^{(p+n-3)/2} \cdot \exp\left[\frac{-x}{2\sigma^2\beta}\right] W_{(-p-2q+n+1)/2,(p-n)/2} \cdot \left(\frac{x}{\sigma^2\beta}\right). \tag{21}$$

Of course, we find again the distributions (8), (10), (12), and (14) for $n = 1$.

Otherwise, if g is the density of the distribution of I and h is the density of the distribution of $A = \sqrt{I}$, then we have $h(x) = 2xg(x^2)$ and $g(x) = (1/2\sqrt{x})h(\sqrt{x})$ (remember that $x \geq 0$). So, for each f being Gamma, Beta second kind, inverse Gamma, or Beta first kind, we have, for the distribution of the amplitude A, four densities $h_1, \ldots, h_4$, respectively. In order to keep consistent notations, we give in Table IV the parameters corresponding to the four possible densities of the distribution of I_1 (which is the same for I_2 and I_3), but the Kolmogorov distance is the distance between the cumulative histogram and the cumulative distribution associated with each h_i. The same is done in Table III, only for the identified distribution.

So, having $E[(I_1)^i]$ for $1 \leq i \leq 4$, we specify the distribution of Λ for each class using the general algorithm presented above. We find Beta of the first kind for the class 1, Beta of the second kind for the classes 2 and 4, and a constant for the class 3. According to Table I, this gives the corresponding distributions of I, which are recalled in Table III.

Then we may notice that the four shapes of the distributions of Λ corresponding to the four classes, which are presented in Fig. 3, are quite different.

The results presented in Table III can then be validated in the following way. As we have the ground truth, we can estimate, for each class, the four parameters γ, p, q, and α. Furthermore, we can also consider that $\lambda\sigma^2$ is constant, which gives an exponential distribution for I. So, for each class we have five candidates for the intensity distribution, and only one is given by the algorithm described above. Is this the best one? To answer this question, we have to define some similarity criterion between a given candidate and the real data. One possible similarity criterion is the Kolmogorov distance defined by

$$d_i^j = \sup_x \left| H_i^j(x) - \hat{H}_i(x) \right| \tag{22}$$

where $\hat{H}_i(x)$ is the cumulative histogram calculated from the data corresponding to the class i and H_i^j is the cumulative distribution of the candidate j (which is defined by the needed parameters estimated from the data corresponding to the class i). For a class i, the five candidates will be K, U, B, W, and exponential distribution, respectively.

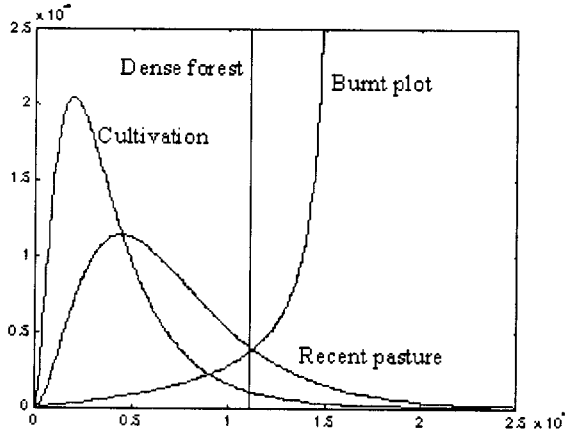

Fig. 3. Distributions of Λ corresponding to the four classes.

TABLE IV
FOR EACH CLASS, ESTIMATED PARAMETERS OF FIVE CANDIDATES AND THEIR KOLMOGOROV DISTANCE TO THE CUMULATIVE HISTOGRAM

	Class 1 (Burnt plot)	Class 2 (Cultivation)	Class 3 (Dense forest)	Class 4 (Recent pasture)
		K law		
α	12.452	1.877	26.789	2.7171
γ	1115,8	2181,6	445.8	2544,9
d_n	**3.049**	**9.658**	**7.026**	**2.71**
		B law		
α	13.45	2.877	27.789	3.719
γ	173020	7687	319930	18798
d_n	**3.239**	**8.168**	**6.838**	**6.731**
		W-U law		
	W	U	W	U
p	1.913	2.78	1.992	2.978
q	0.205	6.919	0.133	31.515
γ	15385	8718.2	12737	73186
d_n	**1.278**	**6.375**	**7.024**	**2.433**
		Exponential law		
$\lambda\sigma^2$	13895	4095	11943	6915
d_n	**2.169**	**47.63**	**5.168**	**26.30**

We present in Table III the estimated parameters and the Kolmogorov distances. We notice that the results given with the general proposed method are consistent with the results of the Table IV. In fact, the method gives W for I of the first class (Table III), and W actually minimizes the Kolmogorov distance (Table IV). The same is observed in the three other cases: the method gives U, Exponential, and U for the classes 2, 3, and 4, respectively (Table III); and the same distributions minimize the Kolmogorov distance (Table IV). Of course, we must not claim that such a validation will occur in all kinds of images. In particular, the use of the Kolmogorov distance is quite arbitrary, and other criteria could give different results. Furthermore, the Maximum Likelihood estimators, as in [17] for the K distribution, could be used to propose some other competing method. However, these results show that situations exist in which the general method proposed is of interest.

V. CONCLUSIONS

In this paper we have presented a novel method for seeking radar image intensity distributions. We assumed that the reflectivity was constant and the number of scatterers random. In such situations the number of scatterers is usually considered as a realization of a Poisson process, defined by a mean λ (called "expected number of scatterers"). The originality of our approach is to assume the expected number of scatterers λ random, with a distribution being in the set of four following possible distributions: Gamma, Beta second kind, inverse Gamma, Beta first kind. We specified how these four distributions induce four calculable densities for the observed intensity. Furthermore, an explicit method of choosing among these four densities from the observed intensity, with the corresponding parameter estimators, has been provided. The new system of intensity distributions so obtained, which includes the classical K law, has then been used to fit real image data, and the fitting results are compared to those obtained for the K law and for the exponential one. These first results show that the new densities considered can be of interest.

One possible perspective is the application of the proposed intensity distribution recognition method to the problem of unsupervised image segmentation. In particular, this could be integrated in the general mixtures estimation methods presented in [7] and [9], which would give, for each class, a density belonging to the KUBW set of distributions. In the case of hidden Markov field and, possibly, numerous correlated sensors, one could envisage some adaptation of the methods presented in [23]. Finally, in more complex situations in which each class may simultaneously contain noise and texture, Markovian models could be used via hierarchical models [18] or pairwise ones [24]. Other possible perspectives are the applications of the proposed intensity distribution recognition method to the radar image synthesis [8] and analysis [3], [6], [25], or to the radar detection of signal in a KUBW-distributed clutter [2], [4], [6].

ACKNOWLEDGMENT

The image of Rondonie was provided by CIRAD SA under the project GDR ISIS. The authors thank A. Bégué for her collaboration.

REFERENCES

[1] M. Abramowitz and I. A. Stegun, *Handbook of Mathematical Functions with Formulas, Graphs, and Mathematical Tables*. New York: Dover, 1972.
[2] R. Barakat, "Direct derivation of intensity and phase statistics of speckle produced by a weak scatterer from the random sinusoid model," *J. Opt. Soc. Amer.*, vol. 71, no. 1, pp. 86–90, 1981.
[3] ——, "Weak scattering generalization of the $\boldsymbol{K}$ density function with application to laser scattering in atmospheric turbulence," *J. Opt. Soc. Amer. A*, vol. 3, no. 4, pp. 401–409, 1986.
[4] E. Conte, M. Longo, M. Lops, and S. L. Ullo, "Radar detection of signals with unknown parameters in $\boldsymbol{K}$-distributed clutter," *Proc. Inst. Elect. Eng. F*, vol. 138, pp. 131–138, 1991.
[5] Y. Delignon, R. Garello, and A. Hillion, "Statistical modeling of ocean SAR images," *Proc. Inst. Elect. Eng., Radar, Sonar Navig.*, vol. 144, pp. 348–354, 1997.
[6] Y. Delignon, "Statistical study of sea surface radar images," Ph.D. dissertation, Univ. Rennes I, France, 1993.
[7] Y. Delignon, A. Marzouki, and W. Pieczynski, "Estimation of generalized mixtures and its application in radar image segmentation," *IEEE Trans. Image Processing*, vol. 6, pp. 1364–1375, Oct. 1997.
[8] R. T. Frankot and R. Chellappa, "Lognormal random field models and their applications to radar image synthesis," *IEEE Trans. Geosci. Remote Sensing*, vol. GE-25, pp. 195–206, 1987.
[9] N. Giordana and W. Pieczynski, "Estimation of generalized multisensor hidden Markov chains and unsupervised image segmentation," *IEEE Trans. Pattern Anal. Mach. Intell.*, vol. 19, pp. 465–475, May 1997.
[10] J. W. Goodman, *Laser Speckle and Related Phenomena*, J. C. Dainty, Ed. Berlin, Germany: Springer-Verlag, 1975.
[11] M. Greenwood and G. U. Yule, "An enquiry into the nature of frequency distributions of multiple happenings, with particular reference to the occurrence of multiple attacks of disease or repeated accidents," *J. Roy. Statist. Soc.*, ser. A, vol. 83, pp. 167–187.
[12] E. Jakeman and P. N. Pusey, "A model for non-Rayleigh sea echo," *IEEE Trans. Antennas Propagat.*, vol. AP-24, pp. 806–814, 1976.
[13] ——, "Significance of $\boldsymbol{K}$ distribution in scattering experiments," *Phys. Rev. Lett.*, vol. 40, pp. 546–550, 1978.
[14] E. Jakeman, "On the statistics of $\boldsymbol{K}$ distributed noise," *J. Phys. A: Math. Gen.*, vol. 13, pp. 31–48, 1980.

[15] J. K. Jao, "Amplitude of composite terrain radar clutter and the $\boldsymbol{K}$ distribution," *IEEE Trans. Antennas Propagat.*, vol. AP-32, pp. 1049–1062, 1984.
[16] N. L. Johnson and S. Kotz, *Distribution in Statistics: Continuous Univariate Distributions I.* New York: Wiley, 1969.
[17] I. R. Joughin, D. B. Percival, and D. B. Winebrenner, "Maximum likelihood estimation of $\boldsymbol{K}$ distribution parameters for SAR data," *IEEE Trans. Geosci. Remote Sensing*, vol. 31, pp. 989–999, May 1993.
[18] P. A. Kelly, H. Derin, and K. D. Hart, "Adaptive segmentation of speckled images using a hierarchical random field model," *IEEE Trans. Acoust., Speech, Signal Processing*, vol. 36, pp. 1628–1641, Oct. 1988.
[19] D. J. Lewinski, "Non stationary probabilistic target and clutter scattering models," *IEEE Trans. Antennas Propagat.*, vol. AP-31, no. 3, pp. 490–498, 1983.
[20] A. Lopes, H. Laur, and E. Nezry, "Statistical distribution and texture in multilook and complex SAR images," in *Proc. IGARSS Symp.*, 1990, pp. 2427–2430.
[21] A. L. Maffett and C. C. Wackerman, "The modified beta density function as a model for synthetic aperture radar clutter statistics," *IEEE Trans. Geosci. Remote Sensing*, vol. 29, pp. 277–283, Feb. 1991.
[22] C. J. Oliver, "Correlated $\boldsymbol{K}$-distributed clutter models," *Opt. Acta*, vol. 32, pp. 1515–1547, 1985.
[23] W. Pieczynski, J. Bouvrais, and C. Michel, "Estimation of generalized mixture in the case of correlated sensors," *IEEE Trans. Image Processing*, vol. 9, pp. 308–311, Feb. 2000.
[24] W. Pieczynski and A.-N. Tebbache, "Pairwise Markov random fields and segmentation of textured images," *Mach. Graph. Vis.*, vol. 9, no. 3, pp. 705–718, 2000.
[25] D. G. Tilley, "Use of speckle for determining the response characteristics of Doppler imaging radar," *Opt. Eng.*, vol. 25, no. 6, 1986.
[26] G. V. Trunk and S. F. George, "Detection of targets in nongaussian sea-clutter," *IEEE Trans. Aerosp. Electron. Syst.*, vol. AES-6, pp. 620–628, 1970.
[27] S. H. Yueh and J. A. Kong, "$\boldsymbol{K}$-distribution and polarimetric terrain radar clutter," *J. Electromagn. Waves Applicat.*, vol. 3, no. 8, pp. 747–768, 1989.

About Off-Axis Radiometric Polarimetric Measurements

Philippe Waldteufel and Gérard Caudal

***Abstract*—Polarization changes for off-axis rays, while a minor effect for narrow-beam antennas, become a significant issue for wide-beam antennas required by synthetic aperture radiometry. This note provides the angle-dependent relationship between upwelling fields and collected signals; results are illustrated by the case of the surface moisture and ocean salinity (SMOS) mission.**

***Index Terms*—Interferometry, polarization, radiometry.**

I. Introduction

The problem of recovering polarized apparent temperature distributions from antenna temperature measurements has been addressed by [1] in the case of a real aperture radiometer. They showed that the antenna couples to both emitted surface polarizations, thus introducing a term involving the product of the polarized and cross-polarized antenna patterns. In the case of synthetic aperture or interferometric radiometers, the problem of measuring polarized temperatures is further complicated because the relationship between radiated and collected Stokes parameters has to be specified for every orientation within the solid angle. In addition, in order to give access to a wide field of view, it is necessary that antenna elements have a wide beam, in such a way that viewing angles with respect to bore sight reach several tens of degrees.

Section II presents the detailed, angle-dependent relationships between brightness temperatures radiated by a surface and linearly polarized signals collected by an interferometric array element. It is found that, whenever these signals are used in a dual-polarization mode, angular zones exist where this relationship cannot be inverted due to a singularity, and therefore radiated horizontal and vertical brightness temperatures cannot be retrieved. These results are illustrated in Section III for a case representative of the future surface moisture and ocean salinity (SMOS) space mission. The simple models used for representing antenna patterns and upwelling temperatures are indicated in Appendix I and II.

Manuscript received January 19, 2001; revised February 14, 2002. This work was supported by Centre National d'Etudes Spatiales (CNES) and Centre National de la Recherche Scientifique (CNRS).

The authors are with Institut Pierre Simon Laplace, CNRS, 78140 Vélizy, France (e-mail: philippe.waldteufel@aerov.jussieu.fr; gerard.caudal@cetp.ipsl.fr).

Publisher Item Identifier 10.1109/TGRS.2002.800236.

II. Transformation of Fields and Stokes Parameters

A. Geometry

When using an interferometric design to image a surface scene, the same antenna array is used to measure the emission signature of any point P on the terrestrial surface within the field of view (Fig. 1). For any such point, therefore, one must perform the geometrical transformation relating the radiated electric fields E_H, E_V to the fields E_X, E_Y measured on the antenna ports. Here, E_H and E_V are the components of radiated electric fields in the usual local reference frame at point P, where horizontal polarization H is perpendicular to the incidence plane, and vertical polarization V is perpendicular to the line of sight in the incidence plane.

We shall consider here the case of a spaceborne interferometer, the antenna of which consists of a set of identical elementary antennas disposed within a plane (the array plane), with bore sights oriented perpendicularly to it. Every antenna has two orthogonal ports X and Y within the array plane. Port X is horizontal and perpendicular to the orbital plane; port Y (as well as the array plane) is tilted by an angle t from the horizontal. The pattern of every elementary antenna is broad, in order to yield access to a wide field of view.

Henceforth, we will define the "antenna frame" as being the spherical reference frame r, θ, ϕ corresponding to the Cartesian frame X, $-Y$, $-Z$ of Fig. 1.

B. Transformation of Electric Fields

The change of reference frame between E_θ, E_ϕ and E_H, E_V has been investigated by Claassen and Fung [1]; they showed that those sets of components are related together through a rotation by an angle ψ around the line of sight direction SP; the rotation angle ψ may be derived through standard geometry. ψ is taken as increasing in the same direction as azimuth ϕ in the r, θ, ϕ reference frame.

If θ_g and ϕ_g are the colatitude and azimuth of point P relative to the satellite position, defined with reference to the geographical frame Sx, y, z, the spherical angles θ, ϕ in the antenna frame and angle ψ may be written as

$$\theta = \operatorname{Arc}\cos\left[\sin t \sin\theta_g \sin\phi_g + \cos t \cos\theta_g\right]$$
$$\phi = -\operatorname{Arc}\sin\left[-\frac{\sin t \cos\theta_g + \cos t \sin\theta_g \sin\phi_g}{\sin\theta}\right]$$
$$\psi = \operatorname{Arc}\sin\left[\frac{\cos t \sin\theta_g - \sin t \cos\theta_g \sin\phi_g}{\sin\theta}\right]. \quad (1)$$